SARCOMERE LENGTH UNIFORMITY DETERMINED FROM THREE-DIMENSIONAL RECONSTRUCTIONS OF RESTING ISOLATED HEART CELL STRIATION PATTERNS

KENNETH P. ROOS
Department of Physiology and the American Heart Association Greater Los Angeles Affiliate Cardiovascular Research Laboratory, University of California, Los Angeles, School of Medicine, Los Angeles, California 90024-1760

ABSTRACT A- and I-band striation positions have been obtained, three-dimensionally reconstructed, and statistically analyzed from the volumes of resting isolated heart cells. Striation patterns from optically discrete subvolumes are imaged along the length of these myocytes with a computer-interfaced optical microscope imaging system. Planar striation maps are reconstructed by the computer from sequentially obtained striation pattern images displaced across the width or depth of the cell in controlled steps. Multiple planar maps are combined to form full three-dimensional (3-D) reconstructions that illustrate the sarcomeric structure and ordering throughout the volume of the cell. These reconstructions demonstrate a high degree of striation registration throughout most regions of cardiac cells. The striation registration is often slightly ($<10°$) skewed across the width or depth of nearly every cell and is occasionally disrupted between adjacent groups of sarcomeres. These disruptions in registration are always associated with the locations of the nuclei. Rigorous statistical analyses indicate small volumetric regions of the cell delineated by these disruptions can have significantly (0.014–0.113 μm) shorter or longer average sarcomere length periodicities. Unlike skeletal muscle "fibrillenstruktur," these data from cardiac cells exhibit no evidence of helical packing schemes for sarcomere order. These observations suggest that the relatively large nuclei displace and disrupt the normal registration of the sarcomeres, which is probably mediated by internal cytoskeletal structures.

INTRODUCTION

The specific alignment and distribution of sarcomeres has not been quantitatively determined within intact, living muscle fibers. The characteristic striation pattern resulting from the interdigitated thick and thin filaments of the sarcomeres from vertebrate muscle preparations appears to be quite uniform and in register. However, sarcomere length nonuniformity has been demonstrated in cardiomyopathic (1) muscle preparations, and in normal skeletal (2–4) and cardiac (5) muscle preparations under various conditions. These nonuniformities can have profound effects on the transmission of force within the muscle cell and therefore upon the overall contractile performance of the preparation.

This study aims to characterize three dimensionally the sarcomere striation pattern of the resting single heart cell or myocyte preparation in an effort to quantify its orientation, registration, and uniformity. This is a necessary first step in the effort to understand more precisely the structural relationship between the cardiac muscle myofilament A- and I-band striations, cellular organelles, the cytoskeleton, and myocardial performance. Cardiac muscle sarcomeres are arranged within each cell in a continuous characteristic "Felderstruktur" (19–21) interspersed and encased by a cytoskeleton (6, 7, 22–26). But there is little quantitative data on the three-dimensional (3-D) uniformity, structure, and organization of the sarcomere striations in living cardiac muscle.

This quantitative structural analysis uses the isolated cardiac myocyte preparation (6–16) and improved optical sectioning light microscopic techniques (13, 16, 17, 18). The cardiac myocyte is a structurally simplified preparation small enough to be monitored completely within the field of view of a high resolution light microscope. Sarcomere striations have been previously recorded from portions of single heart muscle cells by direct optical microscopy with cine film (12), TV (9–11), or solid state (12, 13–16) detectors. The recent applications of optical sectioning microscopy and 3-D image reconstruction techniques (13, 16, 17, 18) have made the monitoring of individual striations possible throughout the volumes of myocytes. These data are then three-dimensionally reconstructed and analyzed for regional sarcomere length periodicity and uniformity. These data are additionally used in the accompanying theoretical article that examines the relationship between striation organization and the light diffraction pattern sarcomere length monitoring technique (27).

METHODS

Isolated Heart Cell Preparations

Isolated heart muscle cells or myocytes (Fig. 2) are prepared by a 15–25-min coronary perfusion (Langendorff) of excised adult rat hearts with a 0.1% collagenase solution. After digestion, the heart is perfused with a Ca^{++}-Tyrode's solution containing, in millimolar: NaCl (130), KCl (4), $MgCl_2$ (1), $NaHCO_3$ (10), NaH_2PO_4 (10.435), $CaCl_2$ (0.25), glucose (5.5), and fatty-acid-free albumin (20 mg/ml), oxygenated with 98% O_2 – 2% CO_2. The Ca^{++}-tolerant cells are obtained by mincing, agitating and filtering the digested heart in perfusate. After a period of equilibration in perfusate containing an increased (1.0–2.5 mM) Ca^{++} concentration, there are a large number of cylindrically-shaped cells that exhibit striking A-, I-band striation patterns and cell nuclei. These cells exhibit the morphological and functional characteristics of intact myocardium and remain quiescent in physiological concentrations of Ca^{++} unless electrically stimulated. Additional details of the cell preparation and perfusate solutions have been previously described (6–8, 14, 15).

Data Acquisition

Fig. 1 illustrates the direct 3-D striation pattern imaging apparatus. A dilute suspension of isolated heart cells is placed in the microscope slide based chamber on the X–Y rotating stage of the light microscope (Carl Zeiss Inc, Federal Republic of Germany). The cells have a roughly ribbon-like shape measuring about 80–150 μm long, 15–30 μm wide, and 10–25 μm thick with one cross-sectional axis being greater than the other. Fresh oxygenated Tyrode's solution circulates slowly through the chamber to maintain cell viability. The cells tend to settle on the bottom of the glass slide chamber with their larger cross-sectional axis parallel to the slide-chamber surface. Thus, the depth dimension is usually less than the width dimension in these cells. Though not securely fastened, they do not move in the slow flowing solution. A single cell is selected that meets the following criteria: ribbon-like shape; clear and distinct striations; no discernible disruptions in the membrane, striations, or intercalated disk regions; and quiescent unless paced electrically with the stimulator in millimeters concentrations of Ca_o^{++}. Data from cells that became spontaneously contractile or went into contracture during the course of the experiment were not used.

Myocyte striation patterns are imaged through the high-resolution (objective N.A. = 1.20, condenser N.A. = 1.40) Nomarski differential interference contrast (DIC) microscope system onto a 1-×-1728 pixel charge-coupled device (CCD) array (Reticon Inc, Sunnyvale, CA) for computer interfaced data acquisition, or into a 35-mm camera (model

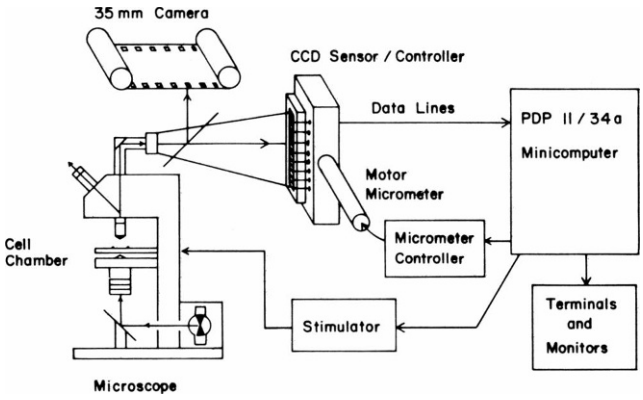

FIGURE 1 Experimental apparatus. The direct 3-D imaging apparatus consists of an high resolution Nomarski differential interference contract (DIC) equipped optical microscope, 35-mm camera, charge-coupled device (CCD) sensing array, and minicomputer. See text for details of operation.

OM-2n; Olympus, Japan) for correlative photomicrographs (Fig. 2). For CCD image acquisition, the DIC of the microscope is always adjusted away from extinction for maximum negative contrast (A-band appears brighter than I-band) on the sensor; for the photomicrographs, the DIC is adjusted closer to extinction for maximum negative contrast on the film (13). Cell image data from the CCD is sequentially digitized and stored in the memory of a minicomputer model (PDP 11/34a; Digital Equipment Corp., Maynard MA) for later analysis. A single 1,728-pixel scan of CCD data represents an imaged cellular subvolume of 86.4 μm in length, 0.053 μm in width, and 1.60 μm in depth as previously described and illustrated (See Fig. 2, reference 13). Additional details of the imaging apparatus (Fig. 1) and the protocols for the acquisition of 3-D striation pattern data have been previously described (13, 14, 16).

The relatively small subvolume of the CCD-acquired myocyte image provides the means to generate a full three-dimensional representation of the striation pattern as previously described (13). Thus, for a given focal plane, a planar striation map (Fig. 3) can be obtained by moving the CCD sensor physically across the width of the cell's image in a series of finite motorized micrometer (Ardel Kinematic Inc., Stratford, CT) controlled steps ranging from 0.34 to 1.01 μm. Similarly, the lateral position of the CCD can be fixed along the width of the cell and the microscope's focus changed by 2.0 to 3.0-μm steps to form a depth planar striation map (Fig. 5). The microscope's focusing mechanism was tested and calibrated with micrometers and an echelon plate; it was unidirectionally linear within 3% of its own calibration markings and exhibited no image foreshortening. By combining these lateral and focal slicing procedures, striation positions throughout the volumes of isolated heart cells can be obtained (Fig. 6). Undoubtedly some regions of the myocyte are missed with the 2.0–3.0-μm focal and 0.34-1.01μm separations used for these studies, but the imaging protocol does provide a reasonable raster-like sample of the striation pattern throughout nearly the entire volume of the myocyte. Finally, most cells are greater in length than the 86 μm imaged in that direction, but relatively short cells are selected from which nearly the entire lengths, and therefore volumes, can be imaged.

Data Analysis

Striation positions are determined from each 1,728-pixel scan of image data by interactive digital processing techniques with a detection error of ±0.05 μm (14, 16). Both A- and I-band striation centroid positions are determined. Sarcomere lengths are calculated from the difference between the centroids of adjacent A-band striation positions. The A-bands are represented by the intensity maxima along a processed intensity profile (Fig. 7, reference 14). Imaging processing eliminates significant variation in peak to peak magnitude (16). There are $N - 1$ sarcomere lengths calculated for each string of N striations.

To reconstruct the cell's striation patterns into planar maps (Figs. 3 and 5) or full 3-D representations (Fig. 6), each striation position is assigned a unique x, y, z coordinate (in micrometers) in accordance with the universal coordinate system described for the accompanying light diffraction study (27). The x coordinate is defined transversely across the width of the cell and the y coordinate is defined along the optical axis through the depth of the cell. The z coordinate is defined as the A-band centroid position from the CCD data scan along the length of the cell. Focal planar maps (Fig. 3) were generated by plotting all the x–z coordinate values for a given y (focal) coordinate. Depth planar maps (Fig. 5) were similarly generated by plotting the y–z coordinates while holding the x (width) coordinate fixed. Full 3-D reconstructions were generated from an entire x, y, z coordinate data set with special graphics hardware and software provided by the IBM (West German Division) IDAMS project. For all types of reconstructions, data points delineate the centroid of each A-band striation position. Solid lines have been drawn in by the computer between adjacent data points to simulate the A-bands. For the full 3-D reconstructions of Fig. 6, each plane's periphery is uniquely defined by solid (upper plane), dashed, dash-dotted, and dotted lines (lower plane). For the edge-view rotation (Fig. 6 *b*), additional simulated striations are drawn with dashed lines by the computer to connect the planes at their edges through the depth of the cell.

Since all of the striation position data for a given cell is stored in the computer as x, y, and z coordinates, subregions of any size within the volume of the cell (from a few sarcomeres to the whole cell) can be selected for statistical analysis of sarcomere periodicity and uniformity. Computer software has been developed: (*a*) to select, by coordinate, sarcomeric regions within the cell's data set; (*b*) to separate and order the sarcomere lengths for presentation as histograms (Fig. 4); (*c*) to calculate the means and standard deviations for each region (Table I); and (*d*) to calculate the statistical significance between the selected regions using two-tailed t tests (Table I). P values in Table I less than 0.05 (*) suggest significant differences between the regions being compared.

The histograms of Fig. 4 present the periodicity distributions from myocytes and a calibration grating by two separate methods. Fig. 4 *a* presents the distribution of the 7,495 sarcomere lengths measured from CCD images of cell number 216 as previously described. Fig. 4 *b* is the sarcomere length periodicity histogram obtained from the direct measurement of low magnification (5,580×) thin-section electron micrographs. Z-line-to-Z-line spacing was measured at regular steps equivalent to 1 μm across the width of the micrographs using the standard line intercept method (a grid of parallel lines oriented along the length of the muscle). This is equivalent to the raster-like CCD data acquisition for all cell image data. The precision of measurement from these low magnification micrographs was ±0.25 mm; this is equivalent to ±0.045 μm (0.25 mm/5,580). These micrographs are prepared from myocytes as described and illustrated in Fig. 6 of Brady and Farnsworth (7). The periodicity histogram of Fig. 4 *c* was derived by CCD imaging a planar map from a precision diffraction grating. This replica grating (Central Scientific Co.) was ruled at 15,000 lines/inch ± 1%, or 1.6933 ± 0.0169 μm/period. The abscissas of all three histograms are drawn to the same scale for direct comparison.

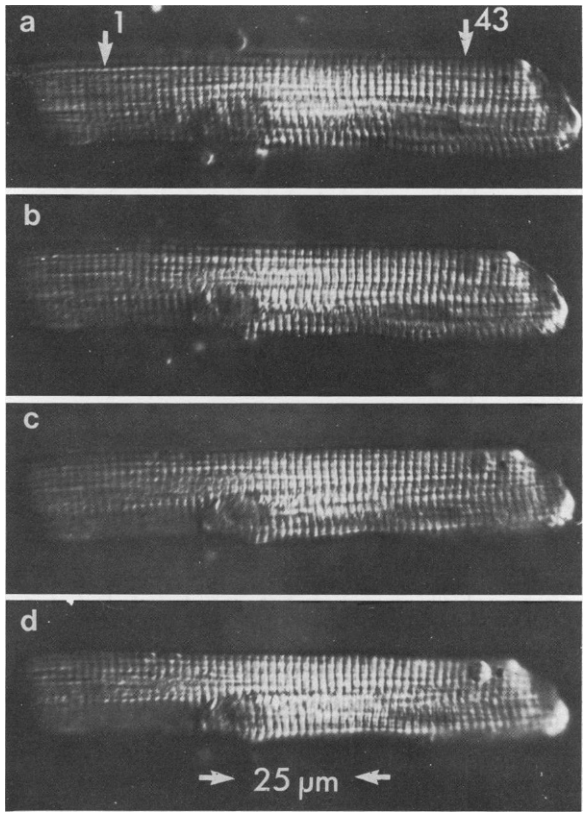

FIGURE 2 Photomicrographs of cell. These photomicrographs illustrate the four adjacent central focal planes from cell No. 216. Micrographs *a–d* are, respectively, at depths 2.5, 5.0, 7.5, and 10.0 μm from the cell surface. The striation pattern and two nuclei are clearly visible at the various depths of focus. The markers on Fig. 2 *a* delimit the longitudinal extent of planar map reconstruction in Fig. 3 *a*.

RESULTS

Planar Sarcomere Registration and Distribution

82 focal planar striation maps and four depth planar striation maps were obtained from 30 resting isolated heart cells. All planar maps have been analyzed for sarcomere length periodicity and uniformity. The data from seven of these cells have been selected for 3-D reconstruction and rigorous statistical analysis on the basis of the following criteria: (*a*) they must contain at least three complete focal planar data sets; (*b*) the lateral separations must be 1.01 μm or less within the focal plane; and (*c*) the focal separations must be 3.0 μm or less. For these seven cells, the number of focal planes ranges from 3 to 5, the lateral separation ranges from 0.34 to 1.01 μm, the focal plane separation ranges from 2.5 to 3.0 μm, and the number of individual sarcomere periodicities measured ranges from 916 to 7,496. This same seven-cell data set has been used as a basis for the following theoretical study of the light diffraction sarcomere length monitoring technique (27).

Figs. 2 and 3 are the photomicrographs and their corresponding focal planar striation maps from the four focal planes of data for cell number 216. This cell contains the largest number of discrete measurements (7,496) with the densest lateral packing of data (0.34 μm). Fig. 2, *a–d* are four photomicrographs taken from this cell at focal (y) coordinate depths 2.5, 5.0, 7.5, and 10.0 μm. The planes above and below those shown in this figure were not in focus implying a total cell depth of 12–15 μm. The focal slicing capability of the high numerical aperture DIC optics is evident in this series of photomicrographs where the two nuclei of the cell are clearly defined in some focal planes, but completely replaced by striations in adjacent planes. One of these nuclei (*right end*) is most prominent in Fig. 2 *a*, while the other nuclei (*left, center*) is most prominent in Fig. 2, *b* and *c*. The striations in these photomicrographs are clearly defined and appear to be uniform in most regions of the cell. However, close examination reveals slight skewing and even complete discontinuities in the striations. Furthermore, these nonuniformities are different in each plane of the same cell. The longitudinal strips superimposed upon the striation pattern that run along the length of the cell are most likely mitochondrial strips that have been shown by EM studies to run parallel to the myofibrils and make up almost ⅓ of the cell volume (19, 20, 28–30). These optically heterogeneous and nonperiodically ordered mitochondria alter the overall translucency and are visualized as longitudinal strips.

Fig. 3, *a–d* are the focal planar map reconstructions of the central 43 striations corresponding to the photomicrographs of Fig. 2, *a–d*. The data points in these planar map reconstructions correspond exactly to their photomicrographs. The arrows of Fig. 2 *a* designate the longitudinal

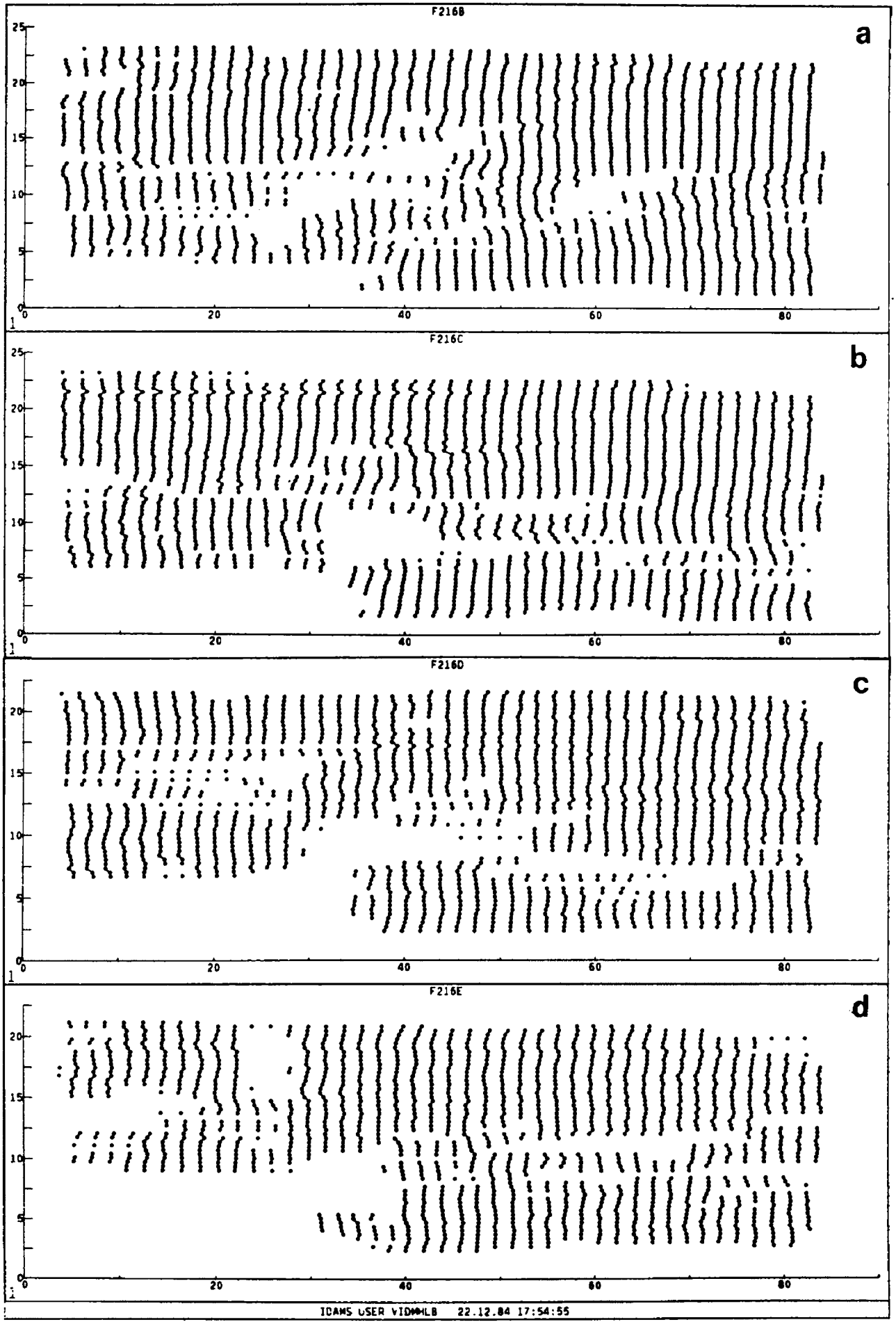
F216B
a
F216C
b
F216D
c
F216E
d
0
5
10
15
20
25
0
20
40
60
80
IDAMS USER VIDMHLB 22.12.84 17:54:55
WIDTH
LENGTH

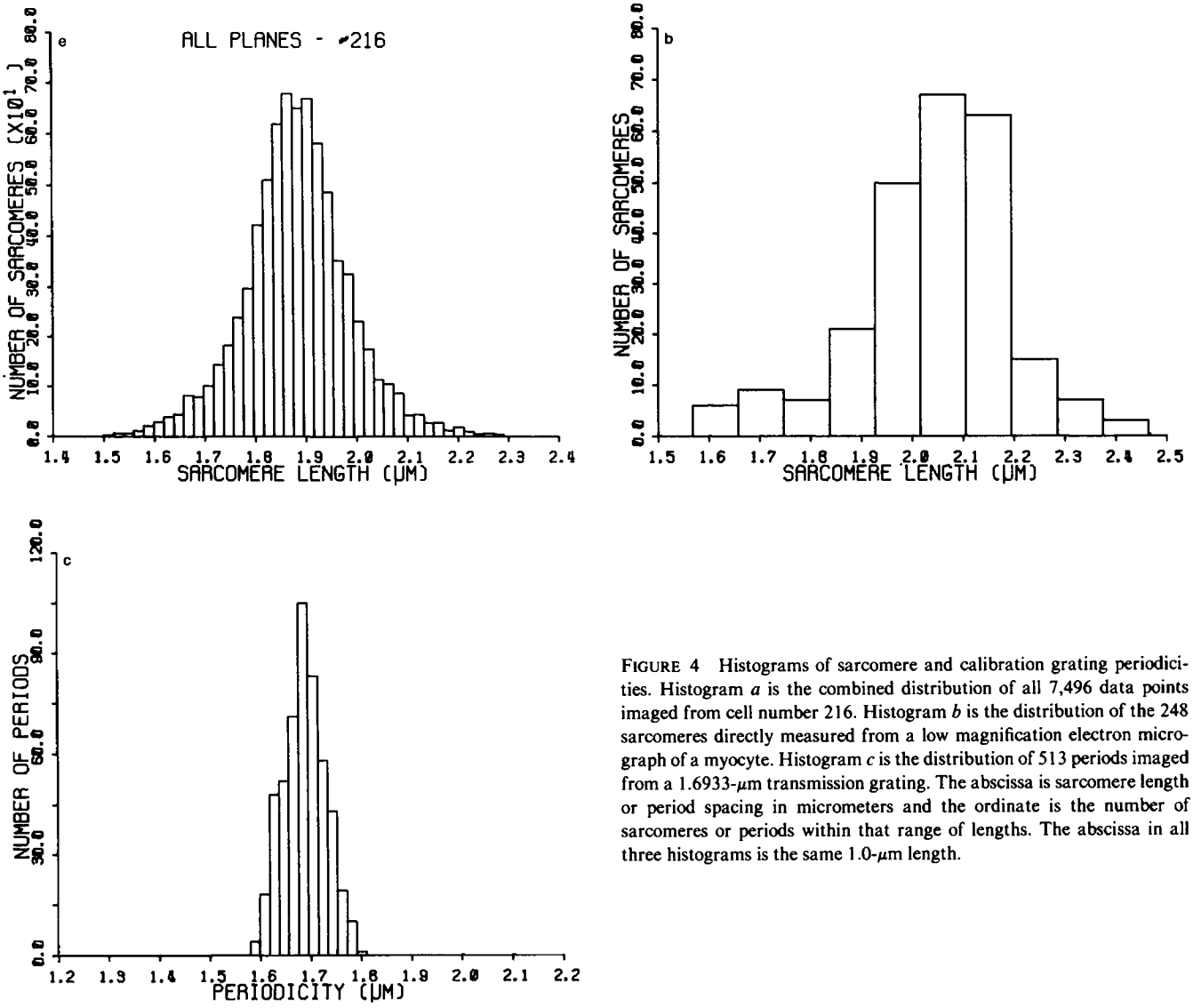

FIGURE 4 Histograms of sarcomere and calibration grating periodicities. Histogram *a* is the combined distribution of all 7,496 data points imaged from cell number 216. Histogram *b* is the distribution of the 248 sarcomeres directly measured from a low magnification electron micrograph of a myocyte. Histogram *c* is the distribution of 513 periods imaged from a 1.6933-μm transmission grating. The abscissa is sarcomere length or period spacing in micrometers and the ordinate is the number of sarcomeres or periods within that range of lengths. The abscissa in all three histograms is the same 1.0-μm length.

extent of the reconstruction; the full imaged width of the cell was reconstructed. These reconstructions more clearly demonstrate the unique striation ordering of each focal plane. Each planar map manifests some degree of striation skewing, pattern discontinuity, longitudinal strips of nonperiodic material, and nuclear gaps. The hole from length (z) coordinates 32–43 and width (x) coordinates 6–12 in Fig 3 *b* is one of the cell nuclei. The other cell nucleus, though partly visible in Figs. 2 *a* and 3 *a* lies slightly above that plane of focus and is not fully reconstructed. Of the 86 focal and depth planar maps obtained, 80 (93%) exhibit significant (>0.1 μm across the width or depth of the cell or ~0.5°) striation skewing. The skewing rarely exceeds 1 sarcomere length across the width or depth of the cell; this corresponds to an approximate maximum skew angle of 10° from the thinnest cells. Yet overall the direction and magnitude of the skewing is variable from region to region with adjacent planes usually demonstrating some consistency. The focal and depth planar maps do not exhibit any rigid ordering, crystalline or helical packing of the sarcomere striations. Also, 35 of the planes from 22 of the cells demonstrate some abrupt type of discontinuity in the striation pattern. Abrupt discontinuities are manifested by longitudinal breaks in the striation pattern where the

FIGURE 3 Focal planar striation map reconstructions. The four (*a–d*) striation map reconstructions correspond directly to the central 43 striations along cell number 216 shown in the four photomicrographs of Fig. 2. Each data point marks one of the 7,496 discrete striation positions determined within these four focal planes. The length and width axes of the cell are indicated and calibrated in micrometers. Striation lines have been reconstructed only between data points from adjacent CCD scans in accordance with the photomicrographs. The lines represent the centroid of the A-band. No lines are drawn between points separated by more than one data scan. The length and width scales are not in exact proportion.

sarcomeres are shifted by up to half of their length. These types of discontinuities are often, but not exclusively, associated with the sarcomeres in series with or adjacent to the nuclei (Fig. 3 *b*). In general, regions of misregistration within the cell appear to be associated with the nuclei.

The histogram of Fig. 4 *a* represents the summation of sarcomere length periodicities from all four planes reconstructed in Fig. 3, *a–d*. The 7,496 individual sarcomere length measurements have a normal distribution about a mean of 1.883 μm; the standard deviation = $\pm$0.105 μm or $\pm$5.58% of the sarcomere length. 95% (2 standard deviations) of the sarcomere lengths measure between 1.670 and 2.092 μm. Histograms representing each planar map of Fig. 3 and those of smaller selected subregions (see Table I) were unique in their specific number of sarcomeres at each length, but all had a normally distributed continuum of measured periodicities. Histograms from the seven cells selected for extended analysis were qualitatively similar with standard deviations ranging from $\pm$0.103 ($\pm$5.57%) to $\pm$0.138 ($\pm$7.36%); see Table I of the following paper (27). Fig. 4 *b* is a histogram of 248 sarcomere lengths measured from a low magnification thin-section electron micrograph of a myocyte. This sample manifests a normally distributed average sarcomere length periodicity of 2.042 $\pm$ 0.152 μm ($\pm$7.44%). Measurements from six other micrographs of myocytes demonstrated normal length distributions with standard deviations ranging from $\pm$0.044 ($\pm$2.34%) to $\pm$0.157 ($\pm$9.90%). Fig. 4 *c* is a histogram from 513 periods measured from a planar map of a diffraction grating. This sample manifests a normally distributed average periodicity calibrated to 1.693 μm with a standard deviation of $\pm$0.044 μm ($\pm$2.60%).

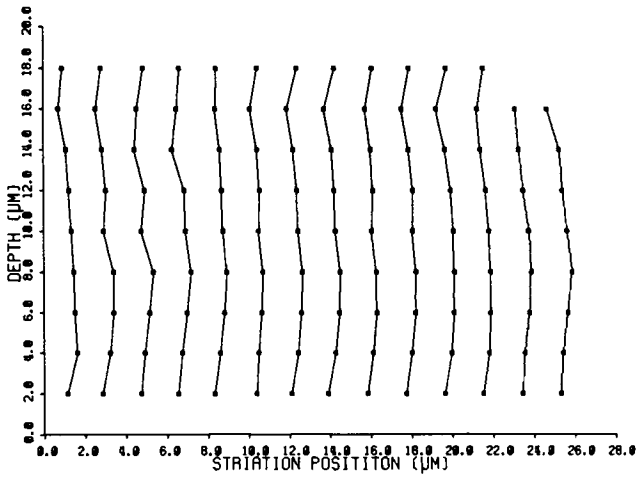

FIGURE 5 Depth planar striation map reconstruction. The striation positions of 14 striations are followed through the depth of cell number 84. The width position was held constant near the middle of the cell and the striations determined from nine focal planes with 2.0-μm separations. The abscissa is the striation position along the length of the cell and the ordinate the focal position through the depth of the cell. The length and width scales are not in exact proportion.

Fig. 5 illustrates the 14 central striations obtained through the depth of a different isolated cell. The data were taken at one width position through the ~20-μm depth of the cell in 2.0-μm steps. As with the focal planar maps of Fig. 3, *a–d*, the striations manifest a slight (<10°) but variable skew. All four depth planar maps obtained demonstrated this type of skewing, but no abrupt discontinuities were seen.

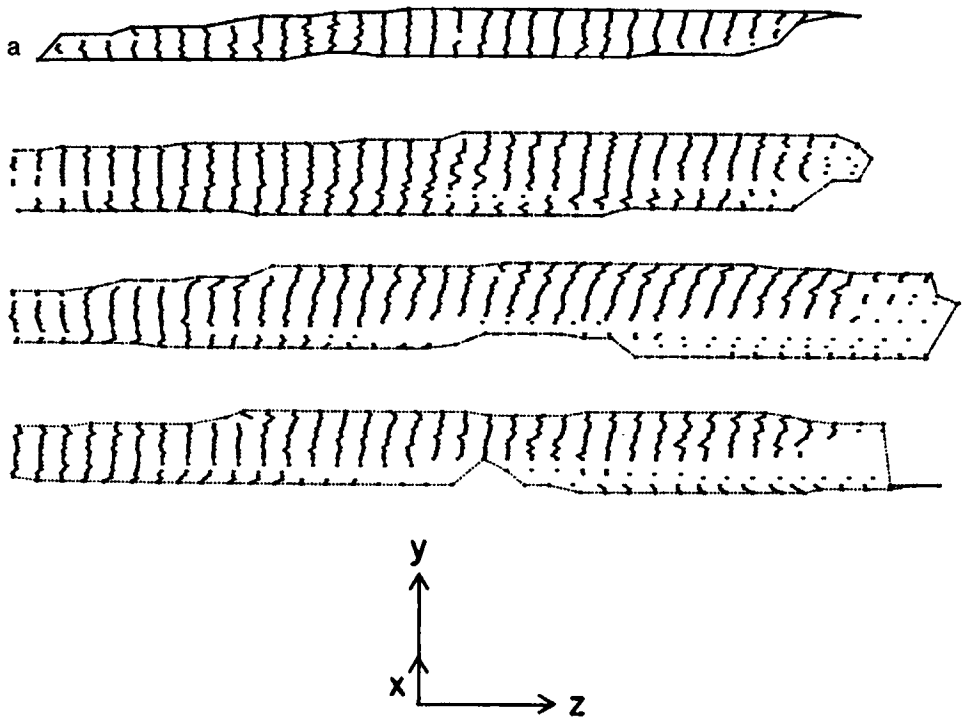

FIGURE 6 3-D reconstructions. A 3-D reconstruction of cell number 135 is presented in two views: (*a* and *b*) an almost side view with rotation coordinates of 85° 0° 0°; (*c*) a top view with rotation coordinates of 0° 0° 20°. Cell number 135 has four planes of data containing 2,158 discrete data points. Adjacent data points are joined by solid lines to simulate striations. Each plane's periphery is uniquely defined: a solid line for the upper plane (Y = 10 μm, a dashed line for the next plane down (Y = 7.5 μm), a dashed-dotted line for the next plane (Y = 5.0 μm), and a dotted line for the lowest plane (Y = 2.5 μm). Reconstruction *b* has additional simulated striations connected vertically between the four planes at their periphery by dashed lines in accordance with their photomicrographs. The length, width, and depth scaling is not in exact proportion due to the perspectives involved in cell rotation.

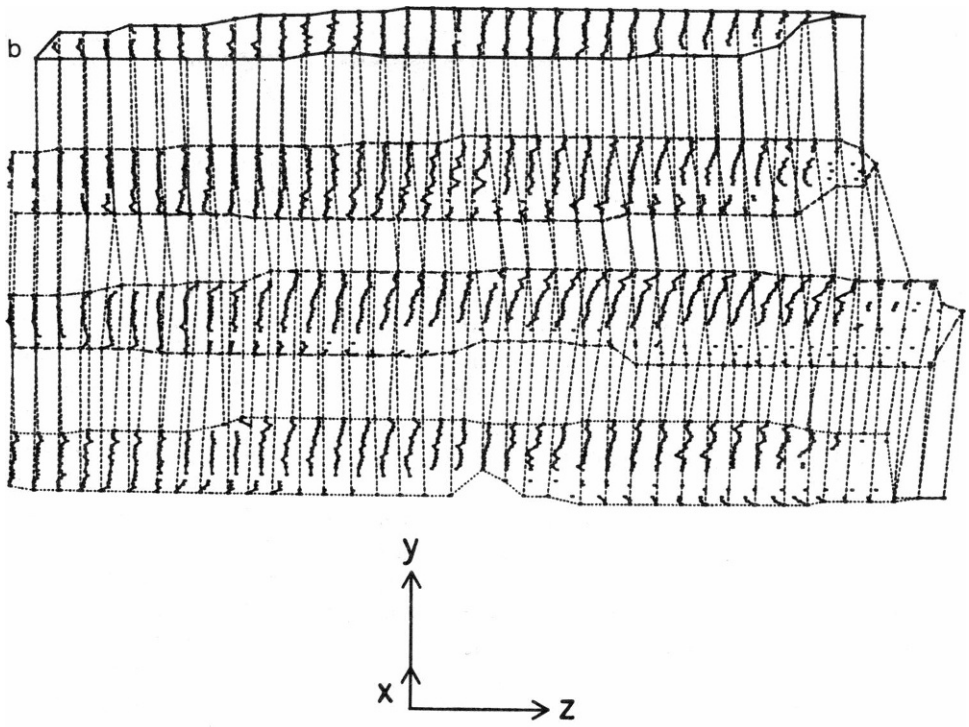

FIGURE 6 Continued

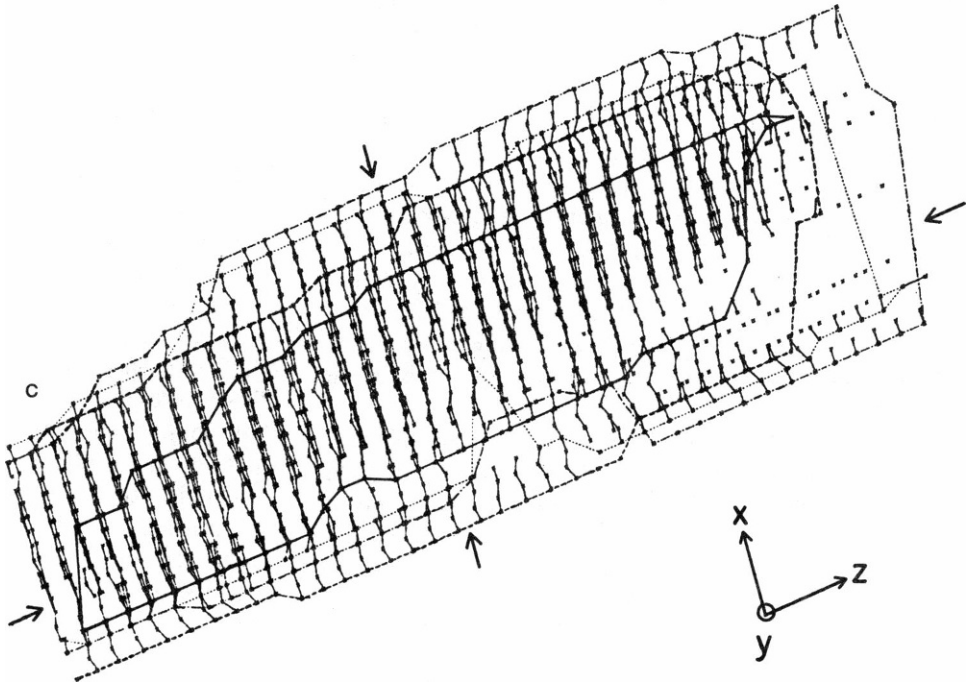

Three-Dimensional Reconstructions

Figs. 6, *a–c* are 3-D reconstructions of the central 43 striations from cell number 135. These reconstructions contain 2,158 striation measurements distributed among four planes. The periphery of each plane is uniquely defined in these figures; a solid line for the upper plane, a dashed line for the next plane down, a dash-dotted line for the next plane, and a dotted line for the lowest plane. As in Fig. 3, *a–d*, each planar striation map of this cell is unique and manifests variable degrees of skewing and discontinuity. Fig. 6, *a* and *b* are rotated so that the optical axis (Y) is nearly vertical and the four planes are viewed from their side. This perspective foreshortens the width of each plane and exaggerates their skewing and discontinuities. Dashed vertical lines are added in Fig. 6 *b* to connect the striations of adjacent planes but only around the cells' periphery. These vertical connections are representative of the variability in skewing through the depth of the cell already demonstrated in Fig. 5. Fig. 6 *c* views the 3-D reconstruc-

tion of Fig. 6 *a* straight down the optical axis (but rotated counterclockwise about that axis by 20°). The striations of all four planes are nearly superimposed throughout most of the cell; the striations of the upper plane tend to be toward the left while those of the lower planes tend toward the right. The lower-right quadrant of the cell has less data points and appears less uniform than the rest of the cell. This is the region where both nuclei are located.

Three-Dimensional Uniformity

Statistical analyses of sarcomere length periodicities from selected planes or subvolumetric regions of the cells indicate large scale uniformity as visually demonstrated in the 3-D reconstructions. For all 30 cells examined, the sarcomere length periodicity was not significantly different between planes (of a given cell) or between an individual plane and the whole cell.

More rigorous regional examination of cell number 135 reconstructed in Fig. 6, *a–c* demonstrate some specific differences. Analysis of 3.0-μm wide longitudinal slices through all four planes along the entire length of the cell (these regions run parallel with the myofilaments) indicate that the lowest 2 slices (x coordinates <6.0 μm, below the arrows in Fig. 6 *c*) are both significantly shorter than the average of the whole cell or any other region. This region is in series with or adjacent to the cell's nuclei. The other longitudinal slices ($x > 6$ μm) are not significantly different among each other or the whole cell.

Similarly, the analysis of 5.0-μm long cross-sectional slices through all four planes at all widths indicate 3 (of 15) regions with significantly longer or shorter sarcomere length periodicities. (These regions are cross-sectional disks 2–3 sarcomeres in length through the entire cell.) Two of these regions (z-length coordinates 40–45 μm, and 50–55 μm) correspond to the beginning and end of nuclei. All other 12 regions are not significantly different from the whole cell and most are not significantly different between themselves.

Table I lists the statistical analyses of periodicity of 8 larger regions within the same cell (number 135, Fig. 6, *a–c*). The columns of Table I list the region, its mean sarcomere length and standard deviation, the number of sarcomeres measured and the comparative statistical P values between each region and the whole cell (left column of P values) and between adjacent regions (right column of P values). Asterisks (*) emphasize data with P values <0.05 that are most likely to be significantly different. The cell has been divided into four quadrants defined by the 6-μm width (x) coordinate and the 35-μm length (z) coordinate; these are defined by the arrows in Fig. 6 *c*. Each quadrant contains all four planes; no statistical differences were found between the planes in each quadrant in this cell. As previously described the lower one-fourth of the cell (both quadrants below the 6-μm width coordinate) is found to be significantly different from the whole cell and the adjacent upper three-fourths. Dividing the cell at the 35-μm length coordinate, the right and left halves are not different from each other or the whole cell. Finally, dividing the cell into four regional quadrants, the two lower quadrants of the cell have the same 1.822-μm average sarcomere length periodicity. This is significantly shorter (0.25–0.35 μm) than the whole cell and the other two quadrants. This cell's data demonstrate alterations in sarcomere length periodicity occurring along the entire length of a cell among a small group of the sarcomeres in series with or adjacent to the nuclei.

TABLE I
REGIONAL UNIFORMITY

Region	Sarcomere length	N	Significance	
	μm		P	
Whole cell	1.847 ± 0.133	2,158	—	—
Lower fourth	1.822 ± 0.158	491	0.001*	0.001*
Upper three-fourths	1.854 ± 0.123	1,667	0.089	
Left half	1.849 ± 0.120	1,053	>0.500	0.500
Right half	1.846 ± 0.143	1,084	>0.500	
Lower-left quadrant	1.822 ± 0.140	255	0.006*	0.001*
Upper-left quadrant	1.857 ± 0.111	798	0.058	
Lower-right quadrant	1.822 ± 0.172	220	0.015*	0.007*
Upper-right quadrant	1.852 ± 0.133	864	0.366	

Most other cells had similar features. In 6 of the 7 cells statistically examined, there were 10 longitudinal regions running parallel to the myofilaments that had significantly different sarcomere length periodicities from the whole cell. The differences between adjacent regions ranged from 0.014 to 0.113 μm. All of these were in series with or adjacent to one or both of the cell's nuclei and were defined by long striation registration discontinuities. Of these 10 regions, 4 had significantly longer and 6 had significantly shorter sarcomere periodicities than the average. Four of the seven cells had significantly different sarcomere periodicities at one end of the cell compared to the other end. These were also usually associated with smaller regions that contained the nuclei. Thus, nearly all (six of the seven) the cells examined contained at least one definable region of significantly shorter or longer sarcomeres which ran longitudinally along the length of the cell. These regions, making up 10–30% of their volume, were always either in series with or adjacent to one or both of the nuclei. However, the sarcomere length periodicity within any definable region was uniform and the striations were essentially in register throughout nearly all the non-nuclear regions.

DISCUSSION

The 2-D planar maps, 3-D reconstructions, histograms, and statistical analyses (Figs. 3–6; Table I) all assist in the characterization of sarcomere registration and length uniformity throughout the volume of isolated cardiac myocytes. The planar maps and 3-D reconstructions (Figs. 3, 5, and 6) provide clear visual information on striation uni-

formity and registration while the histograms and statistical analyses (Figs. 4; Table I) address sarcomere length periodicity. As a whole, these studies have found uniform and well-ordered striation patterns in cardiac myocytes with no evidence for the large scale helical organization characteristic of skeletal muscle fibers (20, 31). However, nearly every cardiac cell had regions of significantly shorter or longer average sarcomere lengths delineated by disruptions in striation registration.

Striation Skewing and Registration

The focal and depth planar maps (Figs. 3 and 5) reveal a high degree of striation registration and uniformity. Most striations can be followed across the entire map despite the many longitudinal gaps and holes representing the nonstriated mitochondrial and nuclear material. However, these striations are subject to skewing or abrupt discontinuities. Nearly every planar map from every cell exhibited a variable amount of striation skewing as manifested by a slight shift in its longitudinal (z direction) position by no more that one sarcomere length (<2.0 μm or $<10°$) from one side of the cell to the other in either the x (width) or the y (depth) directions. These shifts in striation position are usually small within each lateral step of the sensor or within the limits of the depth of focus. Furthermore, the magnitude and direction of this skewing is quite variable.

The planar maps also demonstrate regions of complete discontinuity where the striation positions shift abruptly. These discontinuous shifts in registration are always associated with one or both of the cell's nuclei. Disruptions in registration are seen in the focal planar maps (Fig. 3) but not in the depth planar map (Fig. 5). Nevertheless, these discontinuities in registration do occur in all cross-sectional directions; they are not detected in the depth planar maps (Fig. 5) due to the microscope's relatively large depth of image influence (1.60 μm) compared to the CCD sensor's imaged width (0.053 μm)—see Fig. 2, reference 13. Electron micrographs (also 2-D planar representations) show similar skewing and discontinuous features (7, 19, 20, 29, 30), but are subject to their own set of preparative artifacts. (The histogram of Fig. 4 *b* illustrates the difficulty in precisely quantifying large numbers of sarcomere periodicities even from electron micrographs.)

These striation registration skewing and disruption features evident in the planar maps are maintained throughout the volumes of the myocytes as demonstrated in the 3-D reconstructions (Fig. 6, *a–c*). As viewed three dimensionally, the striation skewing likely arises from the displacement of the sarcomeres by the nuclei and large longitudinally oriented groups of mitochondria. Similarly, the long range disruptions in striation registration adjacent to the nuclei indicate a complete separation of the sarcomere continuum over nearly the entire length of the cell. These 3-D skewing and discontinuity observations suggest that the myofibrils bend around and are separated by the relatively large (compared to other noncontractile organelles) nuclei. Electron micrographs (7, 19, 20, 29, 30) confirm that large amounts of mitochondria often fill the gap separating the two regions along the length of the cells. Furthermore, there is no evidence of any crystalline or helicoid packing schemes of sarcomeres (20, 31) in this cardiac tissue. Unlike the myofibrils ("Fibrillenstruktur") of skeletal muscle, the contiguous "Felderstruktur" of cardiac cell sarcomeres does not appear to manifest any rigid large scale organization (19, 20). This is consistent with overall syncytial organization of heart cells as opposed to the longitudinal organization of cells in skeletal muscles.

Sarcomere Length Periodicity and Distribution

With reference to the planar maps and 3-D reconstructions, average sarcomere length periodicities and distributions were calculated and compared between small x, y, z planar slices and structurally distinct regions of each cell (Table I). Most regions within the volume of myocytes do not have significantly different average sarcomere lengths. This is reflected by the nearly identical mean length of most regions analyzed (regardless of the degree of skewing) and the 3-D striation registration seen in most of Fig. 6 *c*. However, nearly every cell has one or two separate regions of sarcomeres (~10–30% of the total cell volume), which have significantly longer or shorter average periodicities (Table I). Since the number of individual sarcomere lengths used in the statistical analyses is large, small changes in average sarcomere periodicity (~1%) can be significant where P is <0.05. Furthermore, these different regions are longitudinally delimited by the abrupt discontinuities in registration. If adjacent groups of sarcomeres have different average lengths and are parallel, it is not possible physically to maintain striation registration along the entire length of the cell. These regional differences were probably missed in previous striation imaging studies of single cells from this and other labs because only a few or single representative samples were obtained by direct optical imaging (9, 10, 14–16, 18) or because the light diffraction monitoring techniques were used (11, 12). It is not possible to compare regionally sarcomere periodicities within cells using those techniques. The data from this current 3-D study does agree with those previous studies in that the myocytes appear to have internally consistent and normally distributed sarcomere periodicity.

As the histograms of Fig. 4, *a* and *b* illustrate, there is a continuum of sarcomere lengths distributed normally about the mean, whetyher they be measured with the imaging system or from electron micrographs. Histograms imaged from smaller regions within the cell also demonstrated normal distributions providing enough points were included in the analysis. All myocyte histograms had similar distributions of lengths though the mean length measured from electron micrographs was subject to considerable variability (presumably preparative artifacts).

The average percentage of deviation from mean sarcomere length was ±6.35% for the seven myocytes optically imaged and ±5.76% for the seven electron micrographs measured (not significant $P < 0.05$). The histogram derived from the calibration grating (Fig. 4 *c*) had a significantly narrower spread. The standard deviation of the grating periodicity was measured to be ±0.044 μm or ±2.60%. This is a little more than the ±1% precision rating of the grating. The difference must be due to either a greater deviation inherent within the grating, or the actual detection limit of the imaging system, or a combination of both factors. Regardless of grating precision, standard deviations of less than ±0.040 μm are rarely observed. This strongly supports the previous evidence that the lower detection limit of the imaging system is on the order of ±0.040–0.050 μm. Therefore, this histogram of the grating (Fig. 4 *c*) is likely to be a good indicator of the instrumentation precision.

The few extremely long or short individual sarcomeres measured by the direct imaging system are probably the result of optical artifact resulting in erroneous centroid analysis. The optical system's detection performance has been rigorously evaluated under controlled conditions (Fig. 4 *c;* reference 13). Though the optical transfer function of the system derived from those evaluations is fixed, specimen induced artifact could be present from these optically heterogeneous myocytes. Only about half the volume of cardiac myocytes consist of striated myofilaments; the remainder is largely nuclei and mitochondria (19, 28–30). The sarcomeres are contiguous throughout the volume of the cardiac cell but are separated by the two nuclei and large quantities of mitochondria running longitudinally (20). The proportion of striated to nonstriated material within the 1.60-μm depth-of-image influence is variable from region to region within and between data scans. Data scans that contain little or no striated material are highly irregular; these are easily identified during the image-processing procedure and left as gaps in the fully analyzed planar maps and 3-D reconstructions. Though every attempt is made to differentiate between striated and nonstriated material during digital image processing, randomly dispersed optical artifacts can occasionally alter the true centroid position determined from the striation pattern. The occurrence of these must be rare since the sarcomere length distribution histogram from myocyte electron micrographs (Fig. 4 *b*) is very similar to those directly imaged from the living cells but is quite different from the calibration grating. The inclusion of any erroneous longer and shorter sarcomere lengths in these statistical analyses has little effect other than a slight increase in the standard deviation.

Structural Organization of the Myocyte

The isolated single heart cell preparation used in these studies is removed from its highly elastic external collagen matrix, but it still has its own internal cytoskeletal structures (1, 6, 7, 22–26). These are the most likely candidates for the maintenance and determination of striation registration and uniformity. These well-documented internal structures are not a direct part of the contractile apparatus and remain intact after high-ionic-strength myofilament removal (6, 7). Cardiac and skeletal muscle cytoskeleton is believed to be made up of various combinations of: (*a*) intermediate filaments consisting of desmin and vimentin (1, 22, 25, 26); (*b*) connecting, core and side-strut filaments of various sizes (23); and (*c*) the extremely large filaments called connectin, or titin and nebulin (24, 26). These cytoskeletal filaments have been shown to run longitudinally through the middle and around each cell, radially through the M-line and Z-disks of each sarcomere, and between the myofibrils in skeletal muscle cells. Specifically in cardiac muscle, the intermediate filaments (primarily desmin) are present in the largest quantity and therefore believed to play the most significant role in the determination of these uniformity and registration parameters. However, the exact quantitative distribution of these cytoskeletal filaments within and between the myofilaments of mammalian cardiac muscle cells has not yet been determined (1, 5–7).

The high degree of sarcomere registration within a majority of each cell's volume suggests significant interfilament connections between sarcomeres. The most likely candidate is the radially oriented cytoskeletal structures running through the Z-disks and M-lines. Lemanski et al. (1) have suggested that defects in the development of the cytoskeleton in cardiomyopathic hamster hearts are responsible for their gross structural disorganization and poor function. In this study's myocytes from normal rats, the observed striation pattern discontinuities (Figs. 2, 3, and 6) and regional sarcomere length differences (Table I) are likely to be due to smaller scale disruption of these cytoskeleton connections by the relatively large nuclei. The lateral displacement of sarcomeres around the noncontractile nuclei would induce the striation misregistration and skewing, and result in the observed alteration of average periodicity.

It is also possible that these observations of regional length nonuniformity are diminished or at least altered when the myocytes are placed in the syncytium of the ventricular myocardium. Differential external stresses from the collagen matrix surrounding each cell and through the various intercalated disk attachments to adjacent cells could alter overall and regional sarcomere length within the cells. Sarcomere uniformity in the syncytium has not been established, so it is not possible to evaluate the magnitude of this problem.

In summary, these data have shown that sarcomere striation registration and length periodicity is quite uniform throughout most regions of isolated heart cells. There is a small proportion of the volume of most cells that have slightly shorter or longer average sarcomere lengths. These regions are delineated by the nuclei and longitudinal

mitochondrial strips. These nonperiodic and noncontractile organelles probably disrupt the internal cytoskeleton that maintains striation registration and regional uniformity. There is no evidence in cardiac myocytes for the large scale helicoid packing scheme characteristic of skeletal muscle.

The author wishes to thank Dr. Allan J. Brady for his many helpful discussions, electron micrographs, and review of this manuscript. I would also like to thank Bradford A. Lubell for his continued assistance in the data acquisition and analysis software. The technical assistance of David A. Brady, Cecilia Duenas, Barbara Erickson, Steven Farnsworth, and Andy Fukudome was invaluable in the preparation of the heart cells and data processing. The 3-D reconstructions were made possible through the IBM (West German Division) IDAMS pilot study and the Office of Academic Computing at UCLA. The software was developed with the kind and patient assistance of Paul Hoffman.

This work was supported by U.S. Public Health Service grant HL29671, American Heart Association, Greater Los Angeles Affiliate grant 695-G1-3, and the Laubisch Endowment to the author; additional support was obtained from U.S. Public Health Service grant HL30828 to Dr. Allan J. Brady.

Received for publication 6 May 1985 and in final form 16 February 1987.

REFERENCES

1. Lemanski, L. F., and Z.-H. Tu. 1983. Immunofluorescent studies for myosin, actin, tropomyosin and α-actinin in cultured cardiomyopathic Hamster heart cells. *Dev. Biol.* 97:338–348.
2. Edman, K. A. P. 1980. The role of non-uniform sarcomere behavior during relaxation of striated muscle. *Eur. Heart J.* 1:49–57.
3. Edman, K. A. P., and C. Reggaini. 1984. Redistribution of sarcomere length during isometric contraction of frog muscle fibres and its relation to tension creep. *J. Physiol. (Lond.).* 351:169–198.
4. Morgan, D. L., and U. Proske. 1984. Mechanical properties of toad slow muscle attributed to non-uniform sarcomere lengths. *J. Physiol. (Lond.).* 349:107–117.
5. Pinto, J. G. 1978. Macroscopic inhomogeneities of the mechanical response of papillary muscle. *Biorheology.* 15:511–522.
6. Brady, A. J. 1984. Passive stiffness of rat cardiac myocytes. *J. Biomech. Eng.* 106:25–30.
7. Brady, A. J., and S. P. Farnsworth. 1986. Length dependence of cardiac myocyte stiffness following extraction with detergent and high salt concentrations. *Am. J. Physiol.* 250:H932–H943.
8. Brady, A. J., S. T. Tan, and N. V. Ricchiuti. 1979. Contractile force measured in unskinned adult rat heart fibers. *Nature (Lond.).* 282:728–729.
9. De Clerck, N. M., V. A. Claes, E. R. Van Ocken, and D. L. Brutsaert. 1981. Sarcomere distribution patterns in single cardiac cells. *Biophys. J.* 35:237–242.
10. De Clerck, N. M., V. A. Claes, and D. L. Brutsaert. 1984. Uniform sarcomere behavior during twitch of intact single cardiac cells. *J. Mol. Cell. Cardiol.* 16:735–745.
11. Krueger, J. W., D. Forletti, and B. A. Wittenberg. 1980. Uniform sarcomere shortening behavior in isolated cardiac muscle cells. *J. Gen. Physiol.* 76:587–607.
12. Krueger, J. W., and B. London. 1984. Contraction bands: differences between physiologically vs. maximally activated single heart muscle cells. *In* Contractile Mechanisms in Muscle. G. H. Pollack and H. Sugi, editors. Plenum Press, New York. 119–134.
13. Roos, K. P. 1986. Three dimensional reconstructions of optically imaged single heart cell striation patterns. *Biophys. J.* 49:44–46.
14. Roos, K. P., and A. J. Brady. 1982. Individual sarcomere length determination from isolated cardiac cells using high-resolution optical microscopy and digital image processing. *Biophys. J.* 40:233–244.
15. Roos, K. P., A. J. Brady, and S. T. Tan. 1982. Direct measurement of sarcomere length from isolated cardiac cells. *Am. J. Physiol.* 242:H68–H78.
16. Roos, K. P., and B. A. Lubell. 1983. High resolution digital imaging and mapping of heart muscle striation patterns. *Proc. Dig. Equip. Corp. Users Soc.* (Fall, 1982):211–218.
17. Agard, D. A. 1984. Optical sectioning microscopy: cellular architecture in three dimensions. *Annu. Rev. Biophys. Bioeng.* 13:191–219.
18. Williams, W. J. 1984. 3-D computer reconstruction of single skeletal muscle fibers. *Biophys. J.* 45(2, Pt. 2):103a. (Abstr.)
19. McNutt, N. S., and D. W. Fawcett. 1974. Myocardial ultrastructure. *In* The Mammalian Myocardium. Glenn A. Langer and Allan J. Brady, editors. John Wiley & Sons, New York. 1–49.
20. Sommer, J. R., and E. A. Johnson. 1979. Ultrastructure of cardiac muscle. *In* Handbook of Physiology, Section 2: The Cardiovascular System, Volume 1: The Heart. R. M. Berne, N. Sperelakis, and S. R. Geiger, editors. 113–186.
21. Streeter, D. D., H. M. Spotnitz, D. P. Patel, J. Ross Jr., and E. H. Sonnenblick. 1973. Fiber orientation in the canine left ventricle during systole and diastole. *Circ. Res.* 24:339–347.
22. Lazarides, E., and D. R. Balzer, Jr. 1978. Specificity in desmin to avian and mammalian muscle cells. *Cell.* 14:429–438.
23. Magid, A., H. P. Ting-Beall, M. Carvell, T. Kontis, and C. Lucaveche. 1984. Connecting filaments, core filaments, and side struts: a proposal to add three new load-bearing structures to the sliding filament model. *In* Contractile Mechanisms in Muscle. G. H. Pollack and H. Sugi, editors. Plenum Press, New York. 307–323.
24. Matsubara, S., and K. Maruyama. 1977. Role of connectin in the length-tension relation of skeletal and cardiac muscles. *Jpn. J. Physiol.* 27:589–600.
25. Price, M. G. 1984. Molecular analysis of intermediate filament cytoskeleton—A putative load-bearing structure. *Am. J. Physiol.* 246:H566–H572.
26. Wang, K. 1984. Cytoskeletal matrix in striated muscle: The role of titin, nebulin and intermediate filaments. *In* Contractile Mechanisms in Muscle. G. H. Pollack and H. Sugi, editors. Plenum Press, New York. 285–303.
27. Roos, K. P., and A. F. Leung. 1987. Theoretical Fraunhofer light diffraction patterns calculated from 3-D sarcomere arrays imaged from isolated cardiac cells at rest. *Biophys. J.* 52:000–000.
28. Eisenberg, B. R., D. S. Bruner, and R. T. Mathias. 1985. Morphometric analysis of ventricular trabeculae and papillary muscles from Guinea Pig. *Biophys. J.* 47(2, Pt. 2):128a. (Abstr.)
29. Page, E., and L. P. McAllister. 1973. Quantitative electron-microscopic description of heart muscle cells: application to normal, hypertrophied and thyroxin-stimulated hearts. *Am. J. Cardiol.* 31:172–181.
30. Robinson, T. F., B. S. Hayward, J. W. Krueger, E. H. Sonnenblick, and B. A. Wittenberg. 1981. Isolated heart myocytes: ultrastructural case study technique. *J. Microsc. (Oxf.)* 124:135–142.
31. Peachey, L. D., and B. R. Eisenberg. 1978. Helicoids in the t-system and striations of the frog skeletal muscle fibers seen by high voltage electron microscopy. *Biophys. J.* 22:145–154.